CC BY

Assessment of atmospheric dynamics in the high Andean region of Chimborazo Province. Evaluación de la dinámica atmosférica en la zona alto andina Provincia-Chimborazo

Jorge Milton Lara-Sinaluisa[1*], Juan Manuel Martínez-Nogales[2], Vanessa Fernanda Morales-Rovalino[3], Sandra Daniela Lara-Avalos[4], Arquímides Xavier Haro-Velasteguí[5]

Abstract

The study evaluates the dynamic conditions of the lower atmosphere in the high Andean zone of the province of Chimborazo, using the Van Ulden-Holtslag model, adapted to the particular altitude and temperature conditions of the area, as well as to the specific soil conditions. Data obtained from the Atillo, Tixán, and Chocaví weather stations, collected hourly between 2018 and 2021, were used for the variables: humidity, pressure, radiation, temperature, and wind speed. In addition, data such as roughness, albedo, air density, Bowen index, and runoff constant were collected. Applying the Van Ulden-Holtslag model, heat fluxes, friction velocity, and, fundamentally, the Obukhov length were calculated to define stability levels according to the Pasquill classification. The results show that, for the years analyzed, at the weather stations (Atillo, Tixán, and Chocaví), the extremely stable (EE) class prevailed in its entirety, with only 2019 at the Tixán and Chocaví stations, as well as 2020 at the latter station, showing a prevalence of neutral (N), moderately stable (ME), and moderately unstable (MI) stability classes, respectively. Atmospheric stability models are essential for predicting the dispersion of atmospheric pollutants and improving public health.

[1] Magíster en Física. Docente Investigador, Carrera de Gestión del Transporte, Escuela Superior Politécnica de Chimborazo ESPOCH, Riobamba-Ecuador. j_lara@espoch.edu.ec, https://orcid.org/0000-0002-3116-5161

[2] Magíster en Física. Docente Investigador, Carrera de Ingeniería Automotriz, Escuela Superior Politécnica de Chimborazo ESPOCH, Riobamba-Ecuador. jumartinez@espoch.edu.ec, https://orcid.org/0000-0002-4860-1548

[3] Master Universitario en Ingeniería Matemática y Computación. Profesor Investigador, Carrera de Mecánica, Universidad Técnica de Ambato UTA, Ambato-Ecuador. vf.morales@uta.edu.ec, https://orcid.org/0000-0001-8844-8544

[4] Maestrante en Master´s Degree Course in Robotics and Automation Engineering, Università della Calabria, Rende-Italia. dannylarav@gmail.com. https://orcid.org/0009-0004-6350-4019

[5] Doctor en Ciencias Técnicas. Docente investigador, Carrera de Física, Escuela Superior Politécnica de Chimborazo ESPOCH, Riobamba-Ecuador. aharo@espoch.edu.ec, https://orcid.org/0000-0003-3391-5082

Corresponding Author*: Jorge Milton Lara-Sinaluisa, Magíster en Física. Docente Investigador, Carrera de Gestión del Transporte, Escuela Superior Politécnica de Chimborazo ESPOCH, Riobamba-Ecuador. j_lara@espoch.edu.ec

Keywords: atmosphere, stability, instability, temperature, variability.

1. INTRODUCTION

The analysis of variables such as humidity, pressure, radiation, temperature and wind speed are essential to determine the stability of the atmosphere. These factors interact in an intricate manner, and a thorough examination of their combined effects can provide valuable information about the atmospheric processes taking place in the area. For example, atmospheric humidity plays a key role in cloud formation and precipitation, while pressure and temperature are closely related to vertical air movements and the development of high and low-pressure systems. In addition, solar radiation and wind speed can influence the temperature distribution and the mixing of air masses in the region [1].

The exploration of atmospheric stability in the high Andean region is of great importance, since it contributes to a better understanding of local meteorological phenomena and allows more accurate forecasting of extreme meteorological phenomena. These events, such as storms, snowfall or frost, can have a substantial impact on both human activities and ecosystems in the area, which underlines the importance of studying atmospheric stability in this specific geographical context [2,3].

In recent years, several studies on atmospheric stability have been carried out by applying the Pasquill stability classes and the Obukhov length together, studies that have addressed the analysis of wind turbines located at two different sites on flat terrain, one with neutral atmospheric conditions and the other with unstable atmospheric conditions; estimation of atmospheric stability from only 3 levels of wind speed measurements; the dependence between fatigue loads of a wind turbine located in an offshore wind farm and atmospheric stability; a new method for quantifying atmospheric stability; review of studies conducted at the Obukhov Institute of Atmospheric Physics of the Russian Academy of Sciences; as well as a Boundary Layer Solar Sounding [4,5].

2. Theoretical Foundations

2.1. Atmospheric stability

Studies on the atmospheric stability and wake attenuation constant of a large offshore wind farm in the Yellow Sea, as well as the dependence of the turbulent dissipation rate stability on the convective atmospheric boundary layer have been deepened, without neglecting the estimation of seasonal atmospheric stability and mixing height using different schemes. Special mention deserves the research about a theoretical model for the tilt angles of structures in stratified boundary layers and its connection of the turbulent scale and the Monin-Obukhov similarity theory [6,7].

A very significant contribution to the study of atmospheric stability is that the stability of the surface layer plays a crucial role in several processes, such as surface energy balance, atmospheric pollution and boundary layer parameterization. These processes largely depend on the interaction between wind speed and temperature observations at different heights, which are obtained from the extensive network of wind towers in China [8], who used a climatic data set to estimate the level of stability at low levels, where key parameter used to classify the degree of stability is the Obukhov length, which is determined by considering the wind speed and temperature at 10 m and 70 m above ground level.

Large eddy simulations are used to assess the degree of similarity of the mean profile within the convective boundary layer (CBL), which is why considerable attention is devoted to ensure that the profiles are not unduly influenced by the sensitivity of the mesh, as well as to mitigate the presence of inertial oscillations during the spin phase of the simulation. As for the non-dimensional gradients φ, representing wind speed and air temperature, it is generally observed that they present a parallel alignment with the Monin-Obukhov similarity in several cases. However, it should be noted that, within each profile, the slope of these gradients turns out to be steeper than expected. This particular trend has been identified and documented in several recent studies by various researchers [9].

The stability of the atmosphere is related to temperature and altitude, resulting in the formation of the ambient temperature gradient. This gradient represents the rate at which the temperature decreases as the air mass ascends in altitude. The measurement of this temperature is made by means of a balloon connected to a thermometer, which records the temperature incrementally during ascent. This recorded temperature gradient is called the ambient temperature gradient. It should be noted that this reference temperature gradient can be compared to the adiabatic dry temperature gradient, which assumes no heat loss and no heat gain. Under adiabatic conditions, an increasing volume of air with a specific temperature behaves similarly to a balloon. It will expand until its density aligns with that of the surrounding air. Dry air is observed to expand at a rate of 9.8 degrees Celsius per 100 meters of altitude [10].

2.2. Indexes for assessing atmospheric stability

Several types of indexes can be used to evaluate atmospheric stability. Among them are the Monin-Obukhov length, the Pasquill stability classes and the Richardson number, The Pasquill stability class becomes unstable as the wind speed decreases and the solar radiation increases. Conversely, during the night, the Pasquill stability class gradually stabilizes as the wind speed decreases and the net negative radiation increases, and the net negative radiation increases [11].

The Obukhov length, denoted as L, is a measure of length. It can be understood as the height above the surface at which the influence of buoyancy is dominant in the mechanical production of turbulence, as opposed to wind shear. Consequently, wind shear tends to have a greater impact on turbulence dynamics compared to buoyancy, particularly in the lower layers. ($z<>L$), where buoyancy effects are practically negligible [12,13].

To study variations in atmospheric stability, mathematical models, which are an abstract and simplified representation of a real-world system, phenomenon or process using mathematical concepts and equations, have been used. These models are used in various scientific disciplines and areas of study to understand, analyze and predict the behavior of complex systems, as well as for the development of research hypotheses with their corresponding experimental methodology and

verification method [14,15], one of these procedures is the Van Ulden - Holtslag model, which in a simplified way, the Obukhov length is determined by the expression:

$$\mathbf{L} = \frac{(\mu_*)^2 \cdot \mathbf{T}}{\mathbf{k} \cdot \mathbf{g} \cdot \boldsymbol{\vartheta}_*} \qquad \text{(Ec.1)}$$

where:

$$\theta_* = \frac{-H_0}{\rho_0 \cdot c_p \cdot \mu_*}$$

therefore:

$$\frac{-z_0}{L} = \frac{B_0}{S_0}$$

So, the left-hand side of equation (1) constitutes a measure of stability based on the surface production of turbulence that is dependent on buoyancy and shear [16].

It should be considered that:

$$B_0 = \frac{g \cdot H_0}{\rho_0 \cdot c_P \cdot T},$$

while:

$$S_0 = \frac{(\mu_*)^3}{k \cdot z_0}$$

The Van Ulden-Holtslag model has a particular approach that takes into account the integral energy balance linked to a specific volume component centered on the area surrounding the vegetation and the adjacent atmosphere [17,18]. A segment of the absorbed energy goes to generate evapotranspiration, a fundamental factor to evaluate, with the objective of converting the result into measurements indicating water evaporation.

This procedure involves a meticulous analysis of the energy distribution within the designated volume, focusing on the intricate interactions between the vegetation canopy and the enveloping atmosphere, to decipher the implications of evapotranspiration on the overall ecosystem dynamics [19].

Model the dynamic conditions of the lower atmosphere in the high Andean zone of the Province of Chimborazo. Collect meteorological data in the study areas (Atillo, Tixán, Chimborazo). To carry out a bibliographic search of the theoretical elements that sustain atmospheric stability. Adjust the mathematical model of Van Ulden-Holstlag for the high Andean zone of Chimborazo Province, considering Pasquill stability classes and Obukhov length.

3. Materials And Methods

The research design adopted a quasi-experimental approach, since an exhaustive analysis of meteorological data from the highest elevations in the high Andean zone of Chimborazo Province was carried out. The data were obtained from the meteorological stations of Atillo (elevation 3467 m; latitude -2.18699; longitude -78.54919); Tixán (elevation 3546 m; latitude -2.15759; longitude -78.76049) and Chocaví (elevation 3642 m; latitude -1.48839; longitude -78.71219), of the Alternative Energies and Environment Group of the ESPOCH. The stations are located in Guamote, Alausí and Guano cantons, respectively.

The data were processed using the Van Ulden-Holtslag model, which is based on the calculation of the Obukhov longitude and which, together with the Pasquill atmospheric stability indices, makes it possible to determine the atmospheric stability of the area. Considering the temporal constraints imposed on this research effort, along with the multiple parameters that were manipulated within a singular variable, it can be postulated that the research exhibits the distinct attributes of a cross-sectional study.

The study population was the high Andean zone of the Province of Chimborazo. Being the study population the high Andean zone of the Province of Chimborazo, which has a maximum altitude of 6310 masl at the summit of Nevado Chimborazo, a minimum altitude of 100 masl in Cantón Cumandá, it was necessary to locate the meteorological stations located at a higher altitude than the average, being considered therefore the stations of Atillo, Tixán and Chocaví whose elevations are of: 3467, 3546 and 3642 masl, respectively, which Presents a variety of climatic floors ranging from the subtropical in Cumandá, at 100 meters above sea level, to the intense cold of the Andes has an area of 196052.68 hectares of moorland, which represents 32.06% of the total territory of the province comprising the cantons Guamote, Guano and Alausí in the Province of Chimborazo-Ecuador (Figure 1).

Figure 1. Cantons Guamote, Guano and Alausí in the Province of Chimborazo-Ecuador.

3.1. Sample size

Weather stations obtain data hour by hour, 365 days a year. Therefore, the sample consisted of all the humidity, pressure, radiation, temperature and wind speed data for the years 2018, 2019, 2020 and 2021, without considering those for the year 2022 due to damage to the wind speed measurement sensor.

3.2. Primary and secondary data collection technique

It is of primary type since the data were obtained directly from the meteorological stations, without leaving aside the process of cleaning them. Based on a secondary type of technique, data collection was carried out from the review of documents with scientific literature in accordance with the topic, which comes, as mentioned in previous sections, from books, magazines and scientific articles, theses, guides and technical standards.

3.3. Instruments for processing collected data

Data acquisition was performed directly from the computer of each weather station. Once the database (with the variables of humidity, pressure, radiation, temperature and wind speed) was available, its preparation was started to ensure the reliability of the results. This process involved reviewing and correcting invalid and duplicate data, as well as compensating for a five-hour time lag. A common challenge in databases is the presence of missing data, which may be the result of sensor failures or calibrations. Therefore, it became necessary to fill in these data gaps. In this way, it was possible to obtain an integral and complete database, essential for the development of this study.

3.4. Data analysis

To apply the Van Ulden-Holtstlag model, a MATLAB code called ESTAB was used, which allowed the calculation of the heat fluxes Qh, Qe, Qg, Ql, the friction velocity uu, Obukhov length L and the stability index In. With the complete database for each of the years 2018, 2019, 2020 and 2021 from the Atillo, Tixán and Chocaví meteorological stations, we proceeded to order the figures day by day to obtain the averages in each of the hours for each of the years. This work was carried out by means of code in R. Both the results of the MATLAB and R work were exported to Excel. With the Excel files the corresponding graphs were elaborated, gathering the averages for each year in each station, obtaining 3 graphs per variable, one for each station.

4. Results And Discussion

4.1. Atmospheric stability in the Atillo area

Figure 2A shows the atmospheric stability at el Atillo station for 2018. that between 00h00 - 07h00 and then between 19h00 - 24h00 the extremely stable stability class (ES) prevails, followed closely by the stable stability class (S). Between 08h00 and 18h00 conditions prevail together: moderately unstable (MU) and neutral (N). which confirms the information, because throughout the year added together the frequencies of classes (S) and (ES) exceed 52% of the total frequencies (6433). However, class (ES) (2138) is almost twice as frequent as class (S) (1190).

Figure 2B shows that from 00h00 - 06h00 and 20h00 - 24h00, in 2019 classes (S) and (ES) prevail together. With a higher value of class (ES). From 07h00 there is a prevalence of the unstable class (U) which slightly decreases until 18h00. The opposite occurs with the moderately unstable class (MU) from 08h00, which starts a sustained growth until 18h00, confirming the prevalence of class (ES) (3392) out of a total of (8744) of the total frequencies of the year.

Figure 2C shows the prevalence of the class (ES) during the periods 00h00 - 07h00 and 19h00 - 24h00 with more than 50% of the frequencies observed in each hour. The frequency of class (ES) (3083), prevails in (Atillo 2020) of the total (8572) observations as shown in Figure 2D. The class (ES) maintains a clear prevalence in (Atillo 2021), observing that in the period 00h00 - 07h00 was slightly decreased, but maintaining the prevalence in the period 20h00 - 24h00. From 08h00 onwards, the prevalence of unstable class (U) began to increase, decreasing until 18h00. The opposite phenomenon occurs with the moderately unstable class (MU), which from 08h00 begins a growth in prevalence until 18h00. The data show the prevalence of class (ES) (3403), followed by class (MU) (1665) and unstable class (U) (1398) out of a total of (8759) observations.

Figure 2A, 2B, 2C, 2D Atmospheric stability at El Atillo station for the years 2018, 2019, 2020 y 2021.

4.2. Atmospheric stability in the Tixán area

For its part during 2018 at the Tixán weather station, Figure 3A, a clear prevalence of the class (ES) can also be observed in the periods between 00h00 - 07h00 and 18h00 - 24h00. However, in this case, the prevalence of the moderately stable (MS) class is also evident in the period from 08h00 to 17h00. The class (ES) with (3419) observations prevail followed by the extremely unstable class (EU) (2213) out of a total of (8638) observations.

With lower values than in the previous cases, the class (ES) maintains its prevalence in the station (Tixán 2019) in the periods from 00h00 - 07h00 and 19h00 - 24h00, Figure 3B. On the other hand, the moderately unstable (MU) and neutral (N) classes maintain their prevalence from 08h00 to 18h00. Overall, during the year, the prevalence corresponds to the neutral class (N) with (2222), followed by the class (ES) with (1913) and the class (MU) (1601) of a total of (8752) observations.

In the periods from 00h00 - 07h00 and 19h00 - 24h00, the extremely stable (ES) class prevails, followed closely by the stable (S) and neutral (N) classes in their order, in (Tixán 2020), Figure 3C. From 08h00 to 17h00, the (MU) class prevails, followed by the neutral (N) class. With prevalence of the extremely stable class (ES) with (1995), followed by classes (N) and (MU) with (1962) and (1576) respectively out of a total of (8779) observations taken in the year.

Classes (S) and (ES) together show prevalence in (Tixán 2021), Figure 3D, in the periods from 00h00 - 07h00 and 18h00 - 24h00. From 08h00 to 17h00, the prevalence is jointly in the moderately unstable (MU) and neutral (N) classes. However, with the data in graph 40-4, it can be clearly established during the year the prevalence of the extremely stable (ES) class with (2051), followed by the moderately unstable (MU), stable (E) and neutral (N) classes with (1246), (1162) and (1133), respectively out of a total of (7391) observations.

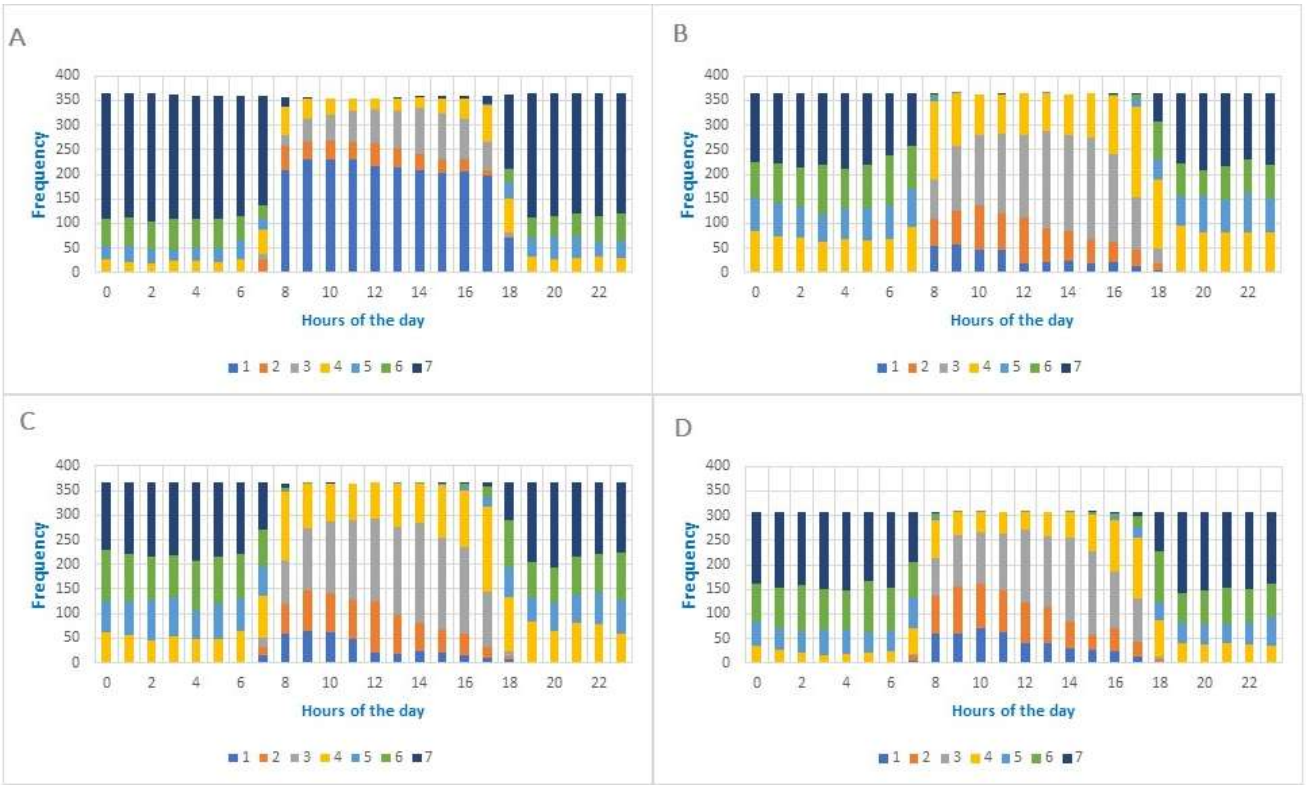

Figure 3A, 3B, 3C, 3D Atmospheric stability at the Tixan station for the years 2018. 2019, 2020 y 2021

4.3. Atmospheric stability in the Chocaví area

In (Chocaví 2018), Figure 4A an indisputable prevalence of the extremely stable class (ES) can be observed in the periods 00h00 - 07h00 and 18h00 - 24h00. From 08h00 to 17h00, the prevalence corresponds to the extremely unstable class (EU), with predominance of the class (ES) (3385), followed by the class (EU) with (2255) of a total of (8759) observations, confirming the results indicated.

Between 00h00 - 07h00 and 19h00 - 24h00 the classes (MU), (S) and (ES) prevail in their order in (Chocaví 2019), Figure 4B Only at 08h00 and 17h00 specifically the neutral class (N) prevails. From 09h00 to 16h00 the prevalence of the (MU) class is clear. With specific data, at the annual level, with the prevalence of classes (MS), (MU), (S) and (N) in their order with (1941), (1924), (1588) and (1504) respectively, out of a total of (8757) observations.

The stable (S) and extremely stable (ES) classes together prevail very clearly in (Chocaví 2020), Figure 4C, in the periods 00h00 - 07h00 and 19h00 - 24h00. From 08h00 to 16h00 the moderately unstable (MU) class prevails, followed by the neutral (N) class. The annual data show the prevalence in order of the classes (MU), (ES), (N) and (MS) corresponding to values of (1677), (1641), (1648) and (1563) respectively out of a total of (8779) observations.

Among all the years analyzed in the 3 meteorological stations, (Chocaví 2021), Figure 4D shows the strongest prevalence of the extremely stable class (ES) during the periods 00h00 - 06h00 and 19h00 - 24h00, as well as the class (EU) in the period from 07h00 to 18h00. The data confirm the information revealing that the extremely stable class (ES) prevails with (5131), then the class (EU) with (3559) of the total of (8723) observations obtained during the year.

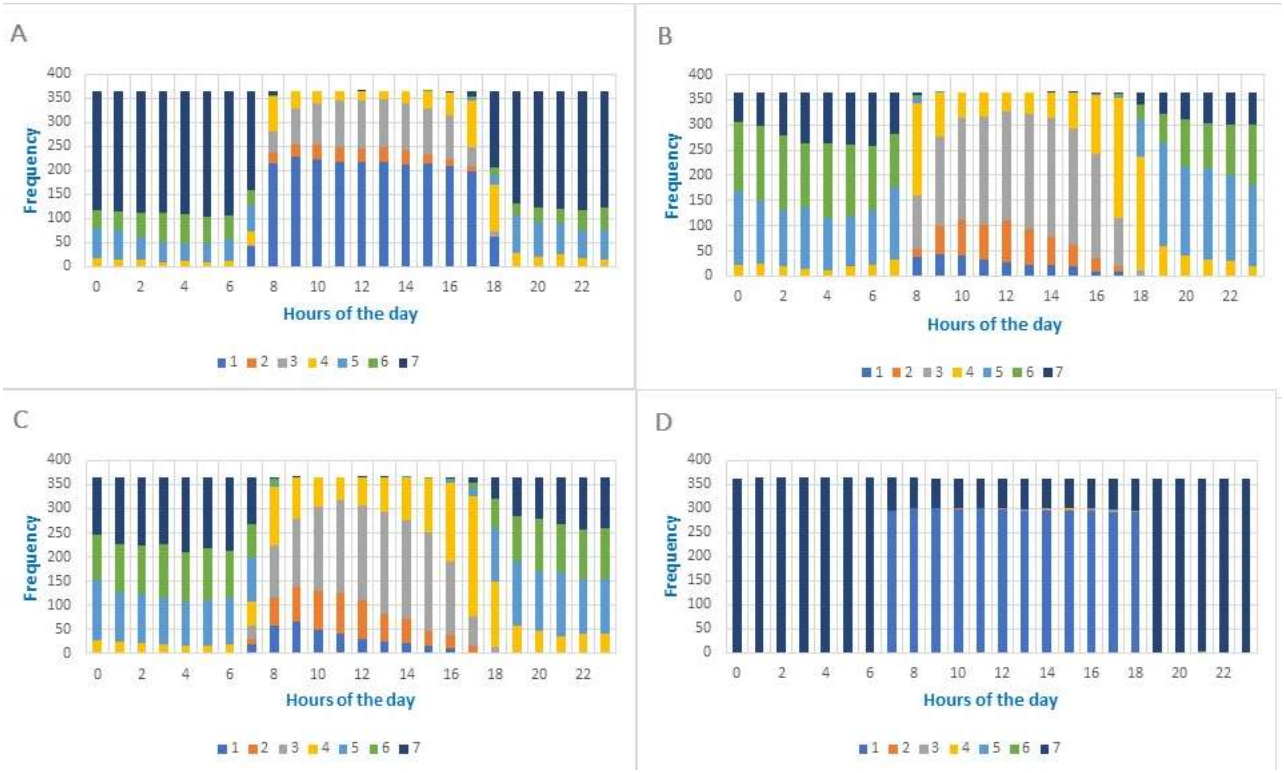

Figure 4A, 4B, 4C, 4D Atmospheric stability at the Chocavi station for the years 2018. 2019, 2020 y 2021

In summary, it can be established that, of years analyzed, in the meteorological stations (4 in each), the extremely stable (ES) class prevails completely. Only during 2019 at the Tixán and Chocaví stations, as well as in 2020 at the latter station, the neutral (N), moderately stable (ME) and moderately unstable (MI) classes prevail, respectively. Thus, in general, the extremely stable class (EE) prevails, followed very closely by the class (E), so that the high Andean zone of Chimborazo Province tends to the stability classes mentioned above.

Discussion

The stability of the atmosphere plays a key role in understanding the intricate nature of local weather patterns, cloud formation, pollutant dispersion, and weather forecasting [20,21]. A comprehensive analysis of this phenomenon by modeling atmospheric stability in the High Andean zone of Chimborazo Province yielded valuable information on several sectors, including agriculture, natural resource management, urban development, and environmental hazard mitigation by detecting areas of atmospheric instability.

Given the unique characteristics found in the data analysis of the Chimborazo Province, which is distinguished by its mountainous terrain and proximity to the equator, the issue of atmospheric stability presents both challenges and opportunities. Factors such as altitude, solar radiation and atmospheric circulation patterns exert a substantial influence on the dynamics of the local atmosphere, which influences variations in precipitation and temperature patterns due to atmospheric instability. Fortunately, in the stations evaluated, this represented a low percentage of the simulated cases [22,23].

Despite the success in the adjustment by modeling atmospheric stability in the High Andean zone of Chimborazo Province, the integration of the atmospheric stability model with other modeling systems is another key aspect. This can be achieved by combining the atmospheric stability model with regional and global climate models to improve long-term predictions. In addition, integration of the model with geographic information systems (GIS) and mapping tools allows visualization and analysis of spatial patterns of atmospheric stability [24,25]. Leveraging the model as a decision support tool for urban planning, emergency management, and environmental risk mitigation is essential for effective governance.

The practical applications of the study of atmospheric stability are the fundamental task should focus on the formulation of mathematical models and computer simulations such as machine learning (ML) or the use of neural networks [26,27], that allow an accurate examination of the physical mechanisms governing atmospheric stability in the region. These models will encompass a variety of variables including temperature, humidity, atmospheric pressure, solar radiation and wind patterns, considering that, the specific geographic and topographic attributes of the Chimborazo Province.

Through the use of advanced modelling methodologies and the analysis of historical and real-time meteorological data, it was possible to generate accurate forecasts related to short- and long-term atmospheric stability. These results are about to have practical implications in several areas, such as: better knowledge of atmospheric stability can facilitate the optimization of agricultural practices, resulting in better crop scheduling [28] better risk management and better preparedness against adverse weather conditions [29].

Likewise, atmospheric stability analysis can contribute to the prediction of precipitation patterns and the assessment of water resource availability [30,31] which are crucial for effective water resource planning and sustainable use, since atmospheric stability models can be instrumental in forecasting the dispersion of air pollutants, allowing the implementation of preventive measures to mitigate negative impacts on public health.

5. Conclusions

The adjusted model made it possible to establish the dynamic conditions of the area, with a predominance of the extremely stable stability class (ES), due to the fact that the low surface temperatures do not allow reaching the energy necessary for convection to occur in the surface layer of the atmosphere, finding that of analysed,

In the meteorological stations, the extremely stable (ES) class prevails completely, highlighting that only during 2019 in the Tixán and Chocaví stations, as well as in 2020 in this last station, the neutral (N), moderately stable (MS) and moderately unstable (MU) stability classes prevail respectively, due to the variation of the meteorological parameters.

The atmospheric instability observed at the Tixán and Chocaví stations during 2018 and 2020 according to the data obtained by applying the Van Ulden-Holstlag mathematical model is due to changes in climatic parameters, particularly wind speed, therefore, it is recommended that those responsible for the control of the meteorological stations pay more attention to the sensors to measure and record this parameter, particularly the one that measures wind speed, and therefore it is recommended to automate the calculation of atmospheric stability in the high Andean zone of the Province of Chimborazo.

Validation of the model for the evaluation of atmospheric stability in the High Andean zone of Chimborazo Province, Ecuador. will be fundamental to quantify the implications of atmospheric stability in various sectors and its relation to changes in precipitation and runoff regimes that affect aquifer recharge, a basic element to effectively manage water resources, as well as its predictive power to model the dispersion of air pollutants under different atmospheric stability conditions and develop mitigation strategies to improve air quality, especially in urban areas.

References

[1] A. P. Van Ulden and J. Wieringa, Atmospheric boundary layer research at Cabauw, Boundary-Layer Meteorol. **78**, 39 (1996).

[2] H. Liu, J. Chen, J. Zhang, Y. Chen, Y. Wen, X. Zhang, Z. Yan, and Q. Li, Study on Atmospheric Stability and Wake Attenuation Constant of Large Offshore Wind Farm in Yellow Sea, Energies **16**, 2227 (2023).

[3] Y. Lv, D. Muñoz-Esparza, X. Chen, C. Zhang, M. Luo, R. Wang, and B. Zhou, Stability Dependence of the Turbulent Dissipation Rate in the Convective Atmospheric Boundary Layer, Geophys. Res. Lett. **50**, (2023).

[4] B. Subramanian, N. Chokani, and R. S. Abhari, Impact of atmospheric stability on wind turbine wake evolution, J. Wind Eng. Ind. Aerodyn. **176**, 174 (2018).

[5] A. Haro-Velasteguí, C. Nieto, N. P. Perugachi-Cahueñas, and M. Parra, Evaluación de la Estabilidad Atmosférica Bajo Condiciones Físicas y Meteorólogicas del Altiplano Ecuatoriano, Rev. Bras. Meteorol. **33**, 336 (2018).

[6] C. Tong and M. Ding, Multi-point Monin–Obukhov similarity in the convective atmospheric surface layer using matched asymptotic expansions, J. Fluid Mech. **864**, 640 (2019).

[7] X. Han, D. Liu, C. Xu, W. Z. Shen, L. Li, and F. Xue, Monin–Obukhov Similarity Theory for Modeling of Wind Turbine Wakes under Atmospheric Stable Conditions: Breakdown and Modifications, Appl. Sci. **9**, 4256 (2019).

[8] J. Li, J. Guo, H. Xu, J. Li, and Y. Lv, Assessing the Surface-Layer Stability over China Using Long-Term Wind-Tower Network Observations, Boundary-Layer Meteorol. **180**, 155 (2021).

[9] M. Heisel and M. Chamecki, On the Departure from Monin–Obukhov Surface Similarity and Transition to the Convective Mixed Layer, Boundary-Layer Meteorol. **190**, 28 (2024).

[10] A. Haro-Velasteguí, J. M. Lara-Sinaluisa, and J. Martínez-Nogales, Small-scale variation of atmospheric dynamics applying chaos theory, case study., Atmósfera **38**, 473 (2024).

[11] K. Nakajima, T. Yamanaka, R. Ooka, H. Kikumoto, and H. Sugawara, Observational assessment of applicability of Pasquill stability class in urban areas for detection of neutrally stratified wind profiles, J. Wind Eng. Ind. Aerodyn. **206**, 104337 (2020).

[12] M. P. Araújo da Silva, F. Rocadenbosch, J. Farré-Guarné, A. Salcedo-Bosch, D. González-Marco, and A. Peña, Assessing Obukhov Length and Friction Velocity from Floating Lidar Observations: A Data Screening and Sensitivity Computation Approach, Remote Sensing.

[13] J. Yano and M. Waclawczyk, Nondimensionalization of the Atmospheric Boundary-Layer System: Obukhov Length and Monin–Obukhov Similarity Theory, Boundary-Layer Meteorol. **182**, (2022).

[14] A. Amores, S. Monserrat, M. Marcos, D. Argüeso, J. Villalonga, G. Jordà, and D. Gomis, Numerical Simulation of Atmospheric Lamb Waves Generated by the 2022 Hunga-Tonga Volcanic Eruption, Geophys. Res. Lett. **49**, e2022GL098240 (2022).

[15] T. Nguyen, J. Brandstetter, A. Kapoor, J. Gupta, and A. Grover, A foundation model for weather and climate., Climax (2023).

[16] Z. Popov, Z. Nagy, G. Baranka, and T. Weidinger, Assessments of Solar, Thermal and Net Irradiance from Simple Solar Geometry and Routine Meteorological Measurements in the Pannonian Basin, Atmosphere.

[17] I. Petenko, G. Casasanta, M. Kallistratova, V. Lyulyukin, C. Genthon, R. Sozzi, and S. Argentini, Kelvin–Helmholtz Billows in the Rising Turbulent Layer During Morning Evolution of the ABL at Dome C, Antarctica, Boundary-Layer Meteorol. **187**, 163 (2023).

[18] S. A. Mata, J. J. Pena Martínez, J. Bas Quesada, F. Palou Larrañaga, N. Yadav, J. S. Chawla, V. Sivaram, and M. F. Howland, Modeling the effect of wind speed and direction shear on utility-scale wind turbine power production, Wind Energy **27**, 873 (2024).

[19] Y. Cheng, M. Zhang, Z. Ziliang, and J. Xu, A new analytical model for wind turbine wakes based on Monin-Obukhov similarity theory, Appl. Energy **239**, 96 (2019).

[20] B. Bochenek and Z. Ustrnul, Machine Learning in Weather Prediction and Climate Analyses—Applications and Perspectives, Atmosphere.

[21] S. Duan, Y. Liu, L. Li, and Y. Pan, Prediction of Atmospheric Carbon Dioxide Radiative Transfer Model based on Machine Learning, Front. Comput. Intell. Syst. **6**, 132 (2024).
[22] C. Pérez Albornoz, M. A. Escalante Soberanis, V. Ramírez Rivera, and M. Rivero, Review of atmospheric stability estimations for wind power applications, Renew. Sustain. Energy Rev. **163**, 112505 (2022).
[23] J. Chen and A. Dai, The Atmosphere Has Become Increasingly Unstable During 1979–2020 Over the Northern Hemisphere, Geophys. Res. Lett. **50**, e2023GL106125 (2023).
[24] Y. Bezyk, I. Sówka, M. Górka, and J. Blachowski, GIS-Based Approach to Spatio-Temporal Interpolation of Atmospheric CO2 Concentrations in Limited Monitoring Dataset, Atmosphere.
[25] H. Muhammad, W. Xuan, M. Wang, and G. Su, Review of spatial scale dispersion models (ATDMs) to simulate environmental dispersion and deposition of radionuclides and the overview of GIS coupling with dispersion models, Int. J. Adv. Nucl. React. Des. Technol. **6**, 256 (2024).
[26] B. Liu, S. Yan, J. Li, Y. Li, J. Lang, and G. Qu, A Spatiotemporal Recurrent Neural Network for Prediction of Atmospheric PM2.5: A Case Study of Beijing, IEEE Trans. Comput. Soc. Syst. **8**, 578 (2021).
[27] L. Zheng, R. Lin, X. Wang, and W. Chen, The Development and Application of Machine Learning in Atmospheric Environment Studies, Remote Sensing.
[28] C. Catalano, L. Paiano, F. Calabrese, M. Cataldo, L. Mancarella, and F. Tommasi, Anomaly detection in smart agriculture systems, Comput. Ind. **143**, 103750 (2022).
[29] A. S. Albahri, Y. L. Khaleel, M. A. Habeeb, R. D. Ismael, Q. A. Hameed, M. Deveci, R. Z. Homod, O. S. Albahri, A. H. Alamoodi, and L. Alzubaidi, A systematic review of trustworthy artificial intelligence applications in natural disasters, Comput. Electr. Eng. **118**, 109409 (2024).
[30] D. B. Nelson, D. Basler, and A. Kahmen, Precipitation isotope time series predictions from machine learning applied in Europe, Proc. Natl. Acad. Sci. **118**, e2024107118 (2021).
[31] J. Cui et al., Global water availability boosted by vegetation-driven changes in atmospheric moisture transport, Nat. Geosci. **15**, 982 (2022).